# IL-8 Triggers Neutrophil Extracellular Trap Formation Through an Nicotinamide Adenine Dinucleotide Phosphate Oxidase- and Mitogen-Activated Protein Kinase Pathway-Dependent Mechanism in Uveitis

Qinxin Shu,[1] Ni Zhang,[1] Yanyao Liu,[2] Xing Wang,[1] Jinquan Chen,[1] Hao Xie,[1] Fuying Pan,[1] Long Zhao,[1] Xuanheng Ding,[1] Yan Wen,[1] Lingda Wang,[1] Wenxi Xie,[1] Jing Lu,[1] Guannan Su,[1] Hui Peng,[1] and Peizeng Yang[1]

[1]The First Affiliated Hospital of Chongqing Medical University, Chongqing Key Laboratory of Ophthalmology, Chongqing Eye Institute, Chongqing Branch (Municipality Division) of National Clinical Research Center for Ocular Diseases, Chongqing, China
[2]Department of Hepatobiliary Surgery, The First Affiliated Hospital of Chongqing Medical University, Chongqing, China

**PURPOSE.** To explore the mechanism underlying IL-8-induced neutrophil extracellular trap (NET) formation in patients with ocular-active Behçet's disease (BD) and the effect of inhibiting NET formation on the severity of inflammation in experimental autoimmune uveitis (EAU) mice.

**METHODS.** The serum extracellular DNA and neutrophil elastase (NE) and IL-8 levels in patients with ocular-active BD, the expression of myeloperoxidase, NE, and histone H3Cit in IL-8–induced neutrophils isolated from healthy controls, and the effects of NETs on HMC3 cells were detected. Female C57BL/6J mice were immunized with IRBP651–670 to induce EAU and EAU mice received intravitreal injection of the CXCR2 (IL-8 receptor) antagonist SB225002 or PBS. The serum levels of extracellular DNA, NE, and keratinocyte-derived chemokine (the mouse ortholog of human IL-8) and expression of myeloperoxidase, NE, and histone H3Cit in mouse retinas were detected. Disease severity was evaluated by clinical and histopathological scores.

**RESULTS.** Serum keratinocyte-derived chemokine expression levels in EAU mice and IL-8 expression levels in patients with ocular-active BD increased. IL-8 notably increased NET formation in a dose-dependent manner through an nicotinamide adenine dinucleotide phosphate oxidase and mitogen-activated protein kinase pathway dependent mechanism. IL-8–induced NET formation damaged HMC3 cells in vitro. Pretreatment with SB225002 notably ameliorated the production of NETs in EAU mice.

**CONCLUSIONS.** Our data confirm that NET formation is induced by IL-8. IL-8–induced NET formation was found to be related to mitogen-activated protein kinase and nicotinamide adenine dinucleotide phosphate pathways. Pretreatment with the CXCR2 antagonist SB225002 alleviated neutrophil infiltration and suppressed NET formation in EAU mice.

Keywords: Behçet, uveitis, interleukin-8, neutrophil extracellular traps

Uveitis often appears as the most common manifestation of Behçet's disease (BD).[1] Chronic bilateral relapsing nongranulomatous panuveitis and retinal vasculitis generally indicate the presence of Behçet's uveitis.[2,3] Ocular-active BD is commonly found in Chinese individuals, especially young adults, with a disturbing relapsing–remitting course.[4,5] BD, ocular active or ocular inactive, is a rare multisystemic inflammatory disorder that is considered attributable to genetic, immunological, and environmental factors. Although its exact etiology remains largely unknown,[6,7] neutrophil hyperactivation has been reported to play a critical role in the pathogenesis of BD.[8]

Neutrophils undergo an inflammatory cell death mechanism called NETosis.[9] This novel form of neutrophil death, distinct from apoptosis, is accompanied by the production of neutrophil extracellular traps (NETs). NETs are released extracellularly by activated neutrophils to capture and destroy pathogens.[10] In addition to the main components, nuclear DNA and histones, especially H3, NETs also structurally consist of various granular proteins such as myeloperoxidase (MPO), neutrophil elastase (NE), and proteinase 3.[11] According to recent research, citrullinated histone H3 (H3Cit) is a crucial component of NETs. Histone citrullination, which is carried out by the histone-specific

enzyme peptide arginine deiminase 4, is one of the crucial stages in NET formation.[12] H3Cit may be used as a particular marker of NET production in peripheral blood and tissue samples.[13,14] NETs participate in the pathogenesis of various ocular disorders, such as diabetic retinopathy,[15] AMD, dry eye,[16] and uveitis. NETs, if dysregulated, may lead to some immune-related diseases, including BD. Circulating serum levels of NETosis markers MPO and NE were reported to be increased in patients with BD. Le Joncour et al.[17] proposed that NETs may be a therapeutic target for preventing or reducing the BD-associated risk of thrombosis. Besides, considerably higher production of NETs has also been reported in the serum of experimental autoimmune uveitis (EAU) mice compared with controls.[18,19] EAU is the most frequently used animal model of EAU and shares common features in clinical and histological aspects with human uveitis. EAU is characterized by massive infiltration of inflammatory cells including neutrophils and macrophages in the eyes.[20,21] We also used EAU as an in vivo model in this study to validate the in vitro results obtained from BD patient-derived cells, which will be elaborated in the Results.

NET formation can be triggered by various stimuli such as nitric oxide, urate crystals, autoantibodies, proinflammatory cytokines (IL-8, IL-6, IL-1$\beta$, and TNF-$\alpha$), and neutrophil interactions with activated endothelial cells or platelets. IL-8 (or CXC chemokine receptor [CXCL]8) attracts and activates neutrophils and directs the migration of chemotactic cells to and recruits neutrophils at the inflammation site.[22] It exerts a range of biological effects via binding to the receptors CXCR1/2, which are expressed by neutrophils.[23] It has been shown that IL-8 levels are closely correlated with disease activity and the presence of clinical manifestations of BD.[24] The sera from patients with BD could enhance the in vitro adherence of normal neutrophils to human endothelial cells and the serum IL-8 level was elevated compared with that in normal controls.[25] One report even implied that serum IL-8 could be a more reliable biomarker of disease activity than erythrocyte sedimentation rate or C-reactive protein in BD.[26] Hence, IL-8 might be a candidate protein that orchestrates neutrophil activity.

However, the specific mechanism underlying NET formation in patients with ocular-active BD has not been elucidated. Herein, we collected samples from patients with ocular-active BD for in vitro studies and used EAU as an in vivo model to explore the mechanism underlying IL-8-induced NET formation. Our study found that IL-8 may trigger the production of NETs via activation of the mitogen-activated protein kinase (MAPK) and nicotinamide adenine dinucleotide phosphate (NADPH) pathways.

## MATERIALS AND METHODS

### Participants

Our study recruited 18 uveitis patients with ocular-active BD that was diagnosed as per the international criteria for BD[27] and 18 age- and sex-matched healthy controls (with no systemic diseases). Ocular-active BD refers to the condition of active intraocular inflammation complicated with other BD traits. Information of the patients with ocular-active BD is shown in Supplementary Tables S1 and S2. All patients exhibited active ocular inflammation when they visited our clinic, as manifested by anterior chamber cells, anterior chamber flare, vitreous haze, and oral ulcers. All patients had not taken any immunosuppressive medicines for at least 1 week before the blood sampling or only had less than

20 mg/d prednisone in the previous week. Other autoimmune diseases, active inflammation, or infections were the exclusion criteria upon patient enrollment. Ethical approval for this study was obtained from the First Affiliated Hospital of Chongqing Medical University. All the procedures were performed as per the principles of the Declaration of Helsinki.

### Preparation of Primary Human Neutrophils

Peripheral blood was obtained from the participants and kept in the BD Vacutainer blood collection tubes (San Diego, CA, USA). Serum samples were obtained through centrifugation at $300 \times g$ for 10 minutes at 21°C. Neutrophils were isolated using the Human Peripheral Neutrophil Isolation Kit (TBD Bio, Beijing, China). The neutrophil layer was slowly collected and mixed with 4 mL of erythrocyte lysate (Thermo Fisher Scientific, Waltham, MA, USA) in a tube (5-minute standing) for removal of erythrocytes. The neutrophils were resuspended in the Gibco RPMI 1640 phenol red-free medium (Thermo Fisher Scientific) containing 2% Gibco fetal bovine blood. The neutrophil purity and cell viability were both more than 90% in our study.

### Isolation and Culture of CD4$^+$ T Cells

A lymphocyte separation medium (TBDscience, Tianjin, China) was used to extract peripheral blood mononuclear cells. CD4$^+$ T cells were isolated from peripheral blood mononuclear cells using CD4 microbeads (Miltenyi Biotec, Bergisch Gladbach, Germany). CD4$^+$ T cells were treated with anti-CD3/CD28 antibody (1 µg/mL, Miltenyi Biotec) for 3 days in 24-well plates ($1 \times 10^6$ cells/mL). The cells were grown in RPMI 1640 complete media including 10% Gibco fetal bovine serum.

**Flow Cytometry.** CD4$^+$ T cells were activated with 1 µL cell activation cocktail containing Brefeldin A (BioLegend, San Diego, CA, USA) for 5.5 hours before being collected, washed, fixed, and permeabilized. The CD4$^+$ T cells were then activated with anti-human IFN-/IL-17 (BioLegend) at 4°C for 1 hours. FlowJo software (version 10.0.7, Treestar, Chico, CA, USA) was used to analyze the flow cytometry data.

### Induction and Treatment of Experimental EAU in Mice

Female C57BL/6 J mice (6–8 weeks old) were provided by ENSIWERER (Chongqing, China). All procedures adhered to the ARVO guideline for animals' use in ophthalmic and vision research and were approved by the Ethics Committee of the First Affiliated Hospital of Chongqing Medical University.

Human IRBP$_{651-670}$ (500 µg) dissolved in PBS (with 20% DMSO) and emulsified with complete Freund's adjuvant (with *Mycobacterium tuberculosis* strain H37Ra, 5 mg/mL) was used for subcutaneous immunization. Intraperitoneal injection of 1 µg pertussis toxin was simultaneously performed. The immunized mice were randomized into the CXCR2 inhibitor (SB225002) (TagerMol, Shanghai, China) group and vehicle group (treated with PBS containing 0.1% DMSO) on the 9th day after immunization. The mice received intravitreal injection of SB225002 in diluent at different concentrations or PBS in an equal volume after anesthetization, followed by the application of antibiotic

ointment for preventing infection. On the 14th day after immunization, the mouse eyes were examined with a slit-lamp microscope by two ophthalmologists independently and the intraocular inflammation was scored as per Caspi's grading criteria.[20]

### Measurement of Extracellular DNA Levels

The peripheral blood of the patients with ocular-active BD and healthy controls was collected and subjected to centrifugation to obtain sera. Serum Extracellular DNA levels were measured using the Invitrogen Quant-iT PicoGreen dsDNA assay kit (Waltham, MA, USA).

### Measurement of Reactive Oxygen Species (ROS)

The obtained neutrophils were resuspended in a medium (1 mL) and preincubated with the fluorescence probe Beyotime DCFH-DA (10 μM; Shanghai, China) for 20 minutes. After being washed with medium three times, the cells were incubated with IL-8 for stimulation. After removal of the medium and washing in PBS three times, the neutrophils were added to a black plate for suspension and then subjected to ROS measurement (excitation, 488 nm; emission, 525 nm) with a Thermo Fisher Scientific microplate reader.

### Quantification of NE and IL-8

To measure NET production, IL-8 and NE levels in human peripheral blood were both detected with ELISA kits (Abcam, Cambridge, UK). KC and NE levels in the blood from C57BL/6J mice were both detected with mouse KC (IL-8) ELISA kits (Yubo, Shanghai, China) and NE ELISA kits (Abcam).

### Total RNA Extraction and RT-qPCR

Total RNA was extracted with Roche TriPure Isolation Reagent (Basel, Switzerland). The extracted RNA population was converted to cDNA by reverse transcription using RT Master Mix & gDNA Digester for qPCR (MedChemExpress, Monmouth Junction, NJ, USA). SYBR Green qPCR Master Mix (MedChemExpress) and Applied Biosystems 7500 RT-PCR System (Waltham, MA, USA) were used for RT-qPCR. The gene expression levels were evaluated and normalized to the housekeeping genes.

### Purification of NETs

A total of $2 \times 10^6$ cells were transferred to each well of the six-well plates, followed by incubation with IL-8 for 4 hours of stimulation. After medium removal and gentle washing, the cell samples were mixed with 500 μL of Gibco RPMI 1640 phenol red-free medium and subjected to vigorous agitation. The samples were then subjected to centrifugation at $500 \times g$ for 5 minutes, and the supernatants were collected in the same way as described elsewhere in this article. Circulating levels and protein levels of DNA/NETs were determined by an Invitrogen Quant-iT PicoGreen dsDNA assay kits and Beyotime BCA protein assay kit, respectively.

### In Vitro Model Using HMC3 Culture

The human microglial cell line (HMC3) was obtained from the American Type Culture Collection (Manassas, VA, USA). The HMC3 cells were maintained in EMEM (with 10% fetal bovine serum, 50 μg/mL streptomycin, and 50 U/mL penicillin) in a humidified incubator. A total of $5 \times 10^5$ cells were seeded in each well of six-well plates for 24 hours and then randomly allocated into the control group, NETs (500 ng/mL) group, and NETs (500 ng/mL) + DNase I (500 ng/mL; Beyotime) group. After corresponding treatment for 24 hours, the cells and supernatants in each group were collected for relevant detection.

### Western Blotting

The procedures were the same as previously described. The obtained proteins of each sample (30 μg) were subjected to Beyotime SDS-PAGE and transferred onto a PVDF membrane. The loaded membrane was blocked in MilliporeSigma TBST solution with 5% (w/v) skim milk. Primary antibodies (1:1000) including anti-IL6 (DF6087), anti-Erk1/2 (AF0155), anti-phospho-Erk1/2 (AF1015), anti-COX2 (AF7003), anti-P38 (AF6456), and anti-phospho-p38 (AF4001) were obtained from Affinity Biosciences (Cincinnati, OH, USA). $\beta$-Actin (AF7018) served as a loading control. The secondary antibodies included HRP-Affinipure goat anti-rabbit or goat anti-mouse IgG (1:10,000; Proteintech, Wuhan, China). The treated membranes were visualized by an ECL assay kit (MedChemExpress). The protein bands were quantified by densitometry through ImageJ software.

### Histopathological Studies

The eyeballs were enucleated from euthanized mice (5 per group) on the 14th day after immunization, and then fixed and immersed in PBS containing 5% glacial acetic acid and 10% formaldehyde. The paraffin-wax embedded tissue underwent serial sectioning (thickness, 4–6 μm) through the papillary–optic nerve axis. After conventional deparaffinization, hydration, and washing, the sections were stained with hematoxylin and eosin. Histological scoring was performed for at least three sections of each eye as per Caspi's criteria. The pathological sections of the retina were evaluated in a blinded manner to determine the degree of retinal inflammatory infiltration and retinal deformation in each mouse.

### Immunofluorescence

To observe the production of NETs, the neutrophils were fixed with 4% paraformaldehyde for 15 minutes, permeabilized with 0.5% Triton X-100 (Sigma-Aldrich, St. Louis, MO, USA) for 20 minutes, blocked with goat serum for 30 minutes, and incubated with anti-MPO (Abcam) and anti-H3Cit (Abcam) at 4°C overnight. Further incubation with Cy3-conjugated goat anti-rabbit IgG (H + L) (1:500, Beyotime) was performed in the dark at room temperature for 30 minutes. Nuclear staining was performed with Beyotime DAPI, and their images were captured with a Leica microscope.

### Statistical Analysis

All the data are presented as the mean ± SD and were statistically analyzed by IBM SPSS 26.0 software (Chicago, IL, USA). Graphical representation was achieved using Graph-Pad Prism 8.0 (La Jolla, CA, USA). The Student *t* test and one-way ANOVA were applied for the comparisons among the data exhibiting a normal distribution and homogeneous variance. *P* values of <0.05 were considered statistically significant.

## RESULTS

### Neutrophils From Patients With Ocular-Active BD Are Primed for NETosis

We first measured extracellular DNA and NE serum levels in patients with ocular-active BD to quantify NET levels (Figs. 1A, 1B). We found higher serum NET levels in patients with ocular-active BD than in age-matched healthy controls. Immunofluorescence studies were performed on neutrophils after isolation and purification. Besides, the levels of H3-cit and MPO (the components of NETs) were detected to confirm NETs (Fig. 1C). Neutrophils from patients with ocular-active BD released more NETs than those from healthy controls in vitro. Taken together, the neutrophils in patients with ocular-active BD were more prone to releasing NETs than those in healthy individuals.

### IL-8 Induces NET Formation In Vitro

IL-8 is a candidate protein for orchestrating neutrophil activity in BD. We found higher serum IL-8 levels in patients with ocular-active BD than in age-matched healthy people in vitro (Fig. 2A). To further explore the effects of IL-8 on NET formation in vitro, we cultured neutrophils isolated from the peripheral blood of healthy individuals with IL-8 (20, 50, 100, and 200 ng/mL) for different durations (1, 2, 3, and 4 hours) and assessed NET levels and stimulation conditions. We found that 4 hours of stimulation with

50 ng/mL IL-8 had the suitable effect (Fig. 2B). In addition, we performed a further investigation of whether NET formation was stimulated by 50 ng/mL IL-8 in contrast with the control by immunofluorescence (Fig. 2C). To further demonstrate NETosis, the levels of H3Cit, MPO, and NE were detected and quantified. The results showed that stimulation with IL-8 could yield higher H3Cit, MPO, and NE levels than the control treatment (Fig. 2D).

### IL-8 Mediates NET Release Via ROS Production

Furthermore, we explored the potential effect of ROS production on IL-8 promotion of NET release. We used the fluorescence probe DCFH-DA to observe the neutrophils from HCs receiving 4 hours of stimulation with IL-8 (50 ng/mL) and found that stimulated neutrophils exhibited increased ROS levels compared with control neutrophils. To illustrate whether ROS affected NET modulation, neutrophils were pretreated with DPI (a specific inhibitor of NADPH oxidase) before IL-8 stimulation, and the results were confirmed by immunofluorescence (Fig. 3A). Under such conditions, DPI suppressed IL-8–induced ROS production (Fig. 3B). DNA/NETs levels significantly declined in neutrophils pretreated with DPI (Fig. 3C). The H3Cit, NOX2, and NOX4 levels decreased upon DPI pretreatment (Fig. 3D), highlighting the role of ROS in these reactions. Altogether, we conclude that IL-8 stimulates NETosis via NADPH oxidase-mediated ROS production.
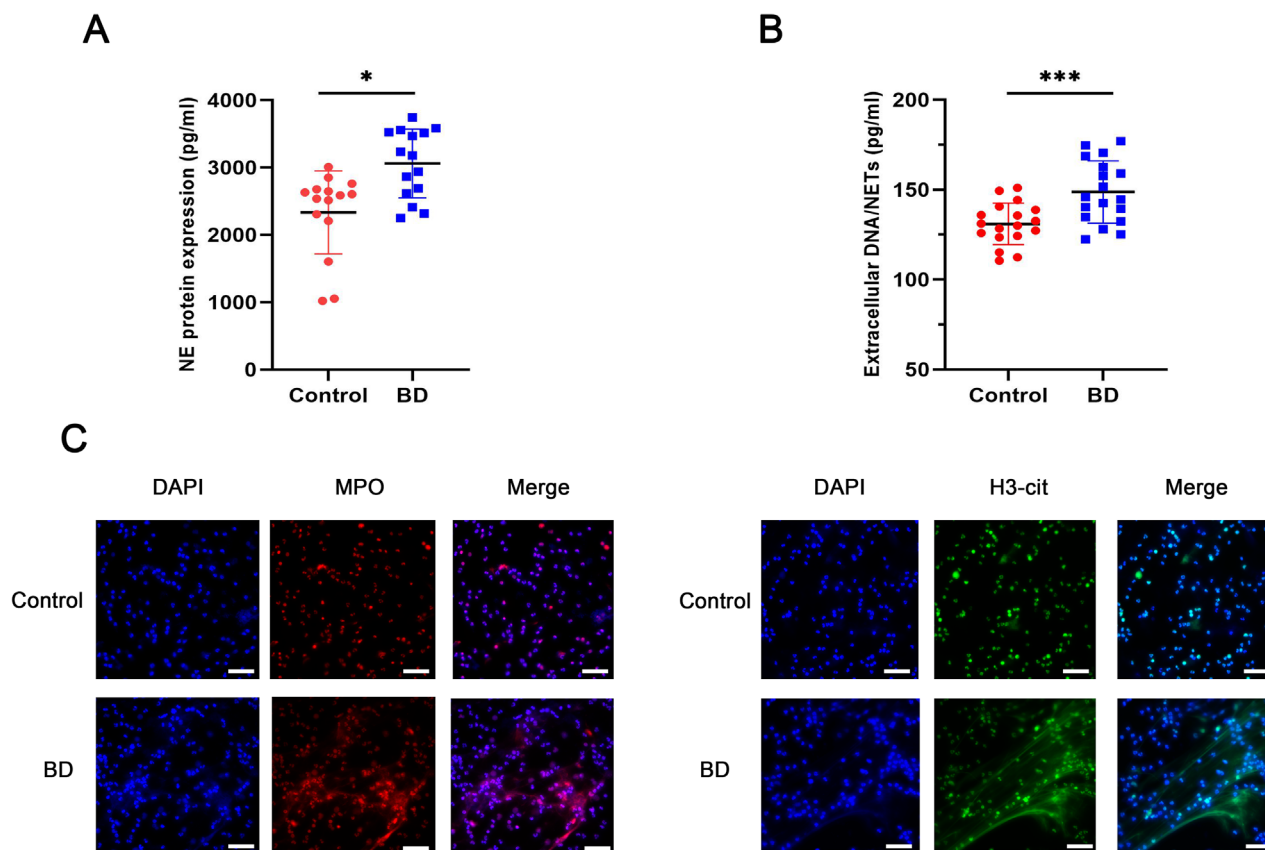


**FIGURE 1.** Neutrophils from patients with ocular-active BD are primed for NETosis. The serum levels of (**A**) NE ($n = 15$ per group) and (**B**) Circulating levels of DNA/NETs of patients with BD and healthy controls ($n = 18$ per group). (**C**) Representative immunofluorescence images of DAPI-labeled DNA and immunolabeled H3Cit and MPO (scale bars, 25 μm). The data were expressed as mean ± SD and analyzed using an unpaired *t* test. *$P < 0.05$, **$P < 0.01$.
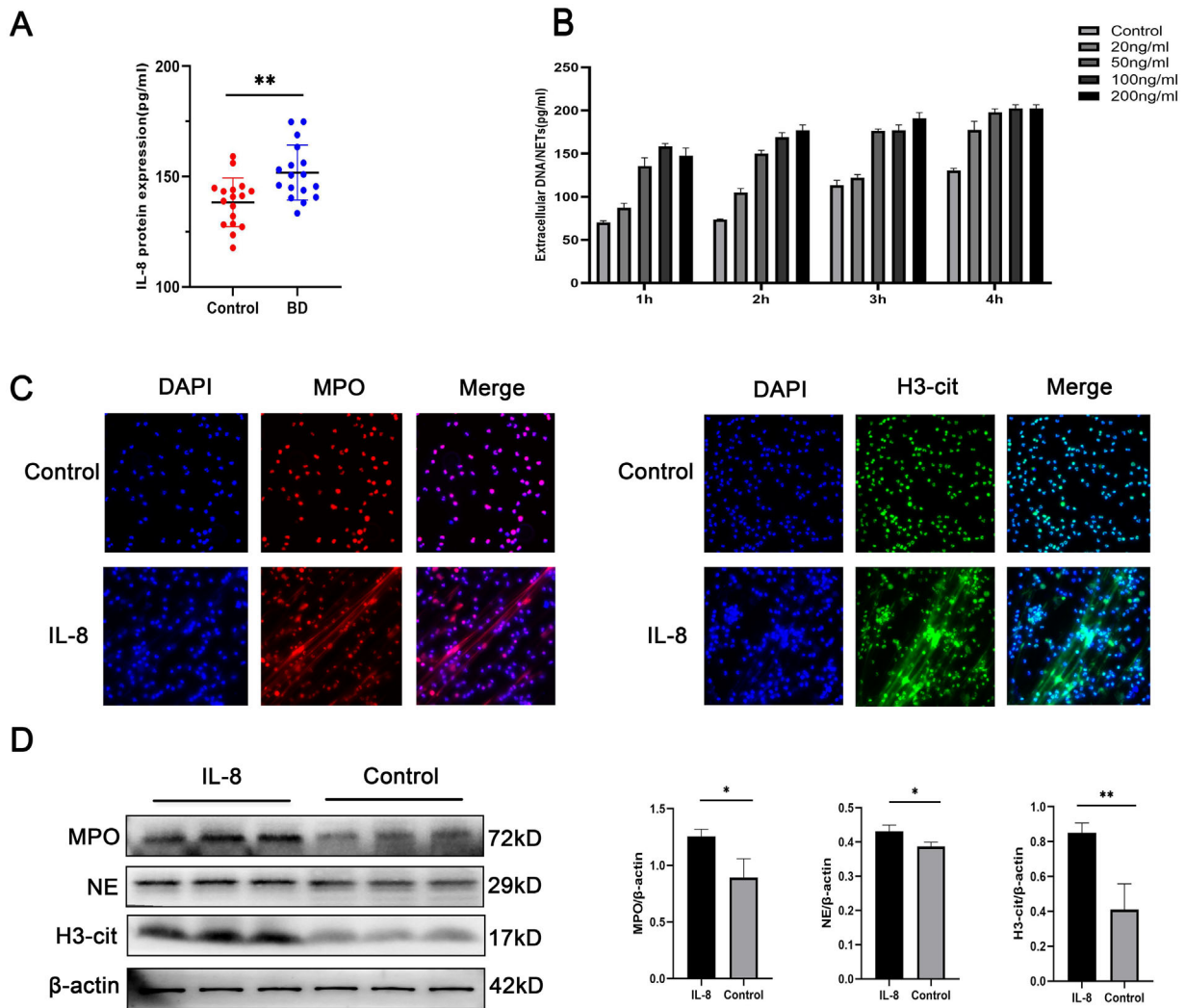
**FIGURE 2.** IL-8 induces NET formation in vitro. (**A**) Comparison between patients with ocular-active BD and healthy controls in IL-8 level ($n = 17$ per group). (**B**) Circulating levels of DNA/NETs levels in the supernatant at various concentrations at various time points. (**C**) Representative immunofluorescence images of DAPI-labeled DNA and immunolabeled H3Cit and MPO of neutrophils incubated with IL-8 (50 ng/mL) or control (scale bars, 25 μm). (**D**) Western blot for H3Cit, NE, and MPO expression in neutrophils incubated with IL-8 (50 ng/mL) or control ($n = 3$ per group). The protein samples were quantified using densitometry through ImageJ software and normalized. The data were expressed as mean ± SD and analyzed using an unpaired *t* test. *$P < 0.05$, **$P < 0.01$.

## MAPK Pathway Participates in NET Release

To explore whether the MAPK pathway was involved in regulating inflammation in vitro in our samples, neutrophils stimulated by IL-8 were treated with the inhibitors of the ERK1/2 and p38 MAPK pathways to assess their effects on the IL-8-mediated induction of NET release. As shown in Figure 4A, the phosphorylation of ERK1/2 and p38 MAPK was significantly raised in IL-8-treated cells, and a 30-minute incubation with their inhibitors (PD98059 and SB203580) was sufficient to inhibit the phosphorylation of ERK1/2 and p38 MAPK. However, no alteration in the total ERK and p38 MAPK levels was found (Fig. 4A). Stimulation with IL-8 and treatment with SB203580 and PD98059 led to a decrease in DNA/NETs levels (Fig. 4B). Similar results were observed through direct microscopy (Fig. 4C). These findings indicate the participation of the MAPK pathway in the NET release.

## NET Formation Triggered by IL-8 Promotes Inflammation in Microglia and CD4^{+} T Cells

We detected the effects of NETs on HMC3 cells and CD4^{+} T cells and observed inflammation in HMC3 cells in the presence of NETs. The protein and mRNA levels of IL-6, TNF-$\alpha$, and COX2 in HMC3 cells were significantly upregulated in the presence of NETs formed by IL-8 stimulation (Figs. 5A, 5B). The addition of DNase I (blocking the effects of the DNA in NETs) partly reversed these inflammatory effects (Figs. 5C, 5D). These findings suggest that the presence of NETs might contribute to the inflammatory response in the microglial cell line. Uveitis is generally considered as a disease mediated by T cells. To determine the effect of NETs on TH1/TH17 cells in vitro an experiment with CD4^{+} T cells co-cultured with these NETs was performed. We found that both the frequency of Th1/Th17 cells and the mRNA levels of IL-17 and IFN-$\gamma$
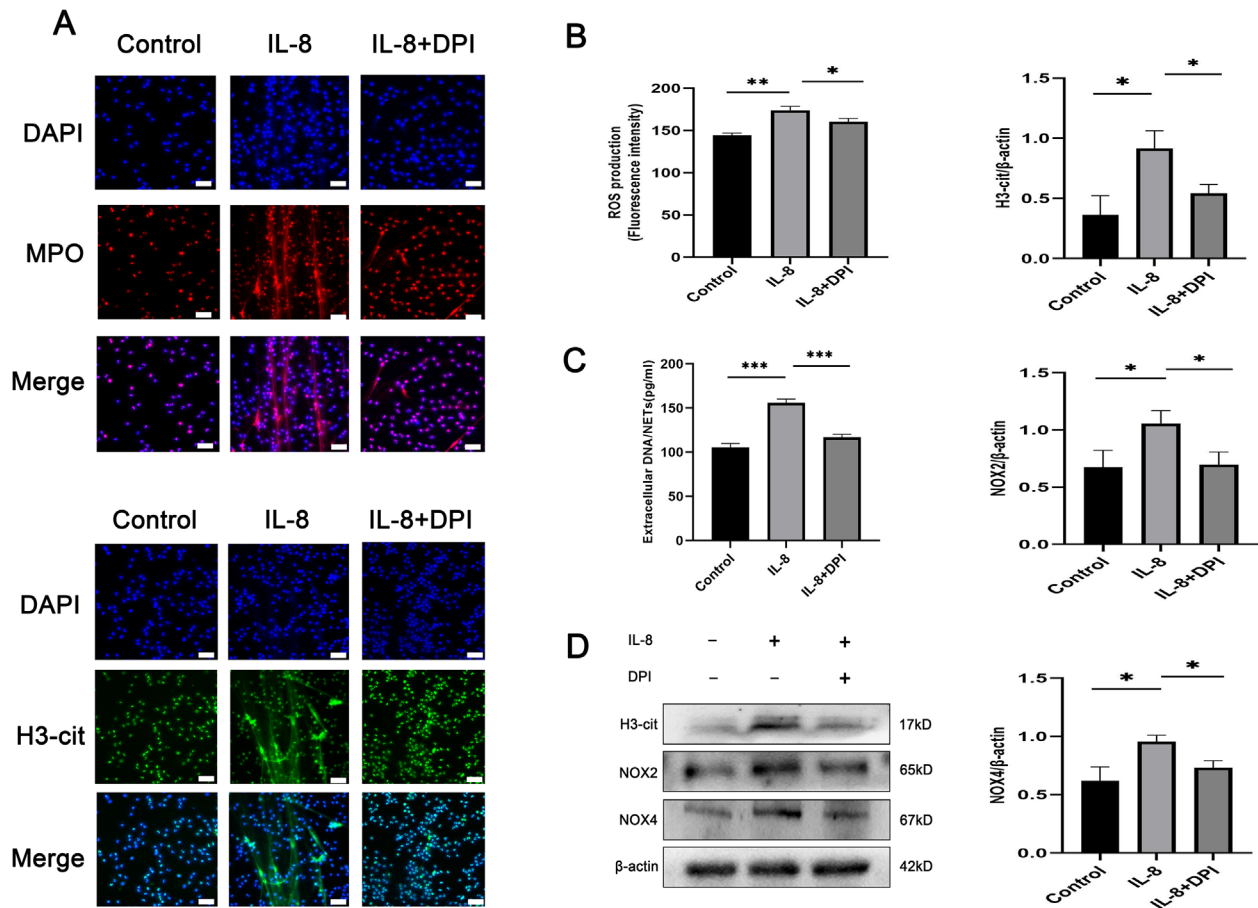
**FIGURE 3.** IL-8 mediates NET release via ROS production. (**A**) Representative immunofluorescence images of DAPI-labeled DNA and immuno-labeled H3Cit and MPO of neutrophils incubated with IL-8 (50 ng/mL) or control in the absence or presence of the ROS inhibitor DPI (10 µM). Scale bars, 25 µm. The measurements of (**B**) ROS levels and (**C**) extracellular DNA indicated the presence of NETs after the above treatment ($n = 3$ per group). (**D**) Western blot for H3Cit, NOX2, and NOX4 expression in neutrophils treated as mentioned elsewhere in this article ($n = 3$ per group). The protein samples were quantified using densitometry through ImageJ software and normalized. The data were expressed as mean ± SD and analyzed using a one-way ANOVA test. *$P < 0.05$, **$P < 0.01$.

were up-regulated by NETs isolated from neutrophils (Figs. 5E, 5F).

## NET Release Is Increased in EAU Mice

The serum levels of extracellular DNA and NE in EAU mice were higher than those in the control mice (Figs. 6A, 6B). Ly6G is a specific neutrophil marker. Significantly higher RNA expression of Ly6G was observed in the retinas of EAU mice than in those of control mice, and we aimed to determine the potential relationship between neutrophil infiltration and retinal inflammation. Therefore, we detected the expression of Ly6G, COX2, IL-6, and TNF-$\alpha$ in EAU mice, and found that all these inflammatory factors were significantly increased (Fig. 6C). Western blot assays revealed a significant upregulation in the protein levels of H3Cit, MPO, and NE in EAU retinas in contrast with the controls (Fig. 6D). Taken together, these results suggest that NETs may cause retinal inflammation in EAU mice.

## SB225002 Improves the Clinical and Histological Manifestations of EAU Mice

Keratinocyte-derived chemokine (KC) is the mouse ortholog of human IL-8. Some literature has shown that the mice express KC, whose biological function is similar to that of IL-8, acting as a key mediator of acute inflammation and neutrophil chemotaxis in mice.[28,29] KC competitively binds to the IL-8 type B receptor and interacts specifically with the mouse homologous receptor mCXCR2.[30] KC can increase the production of proinflammatory mediators by attracting neutrophils to the injured site. Because the serum KC level was significantly upregulated in EAU mice in contrast with the controls (Fig. 7A), we wanted to investigate whether this phenomenon depends on CXCR2. SB225002 is a potent and selective CXCR2 antagonist that selectively inhibits IL-8 and KC-mediated neutrophil migration. We injected SB225002 into the vitreous cavity of EAU mice to verify whether it could alleviate the formation of NETs. On the 14th day after immunization, the SB225002-treated EAU mice had significantly decreased clinical scores compared with the vehicle group. Their histopathological sections suggested its inhibitory effect on the inflammatory activity of EAU in a dose-dependent manner (Figs. 7B, 7C). Furthermore, Western blot analyses of the mouse retinas obtained on the 14th day after immunization were performed to explore whether SB225002 could regulate the formation of NETs and the subsequent inflammatory response. The results showed a significant decrease in H3Cit, NE, and MPO levels and the phosphorylation of ERK1/2 and p38 MAPK in the retinas of SB225002-treated EAU mice compared with the vehicle-
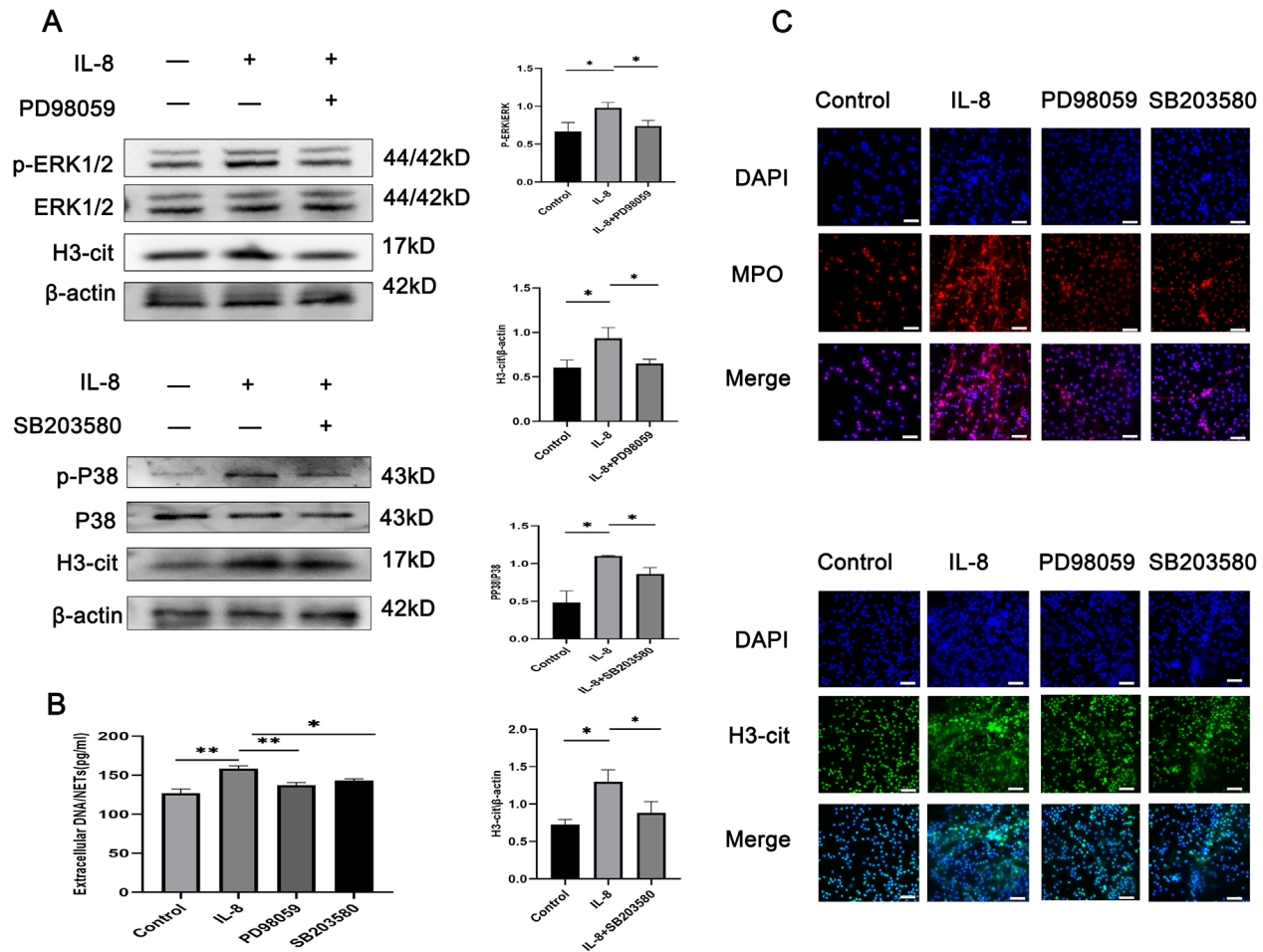
**FIGURE 4.** The MAPK pathway participates in NET production. (**A**) Western blot for the phosphorylation of H3Cit, p38 and ERK1/2 in neutrophils pretreated with the inhibitors SB203580 (20 µM/L) or PD98059 (10 µM/L) for 0.5 hours and incubated with IL-8 (50 ng/mL) or the control for 4 hours ($n = 3$ per group). The protein samples were quantified using densitometry through ImageJ software and normalized. (**B**) The measurements of extracellular DNA levels indicated the presence of NETs after the above treatment ($n = 3$ per group). (**C**) Representative immunofluorescence images of DAPI-labeled DNA and immunolabeled H3Cit and MPO of neutrophils treated as mentioned above ($n = 3$ per group). The data were expressed as mean ± SD and analyzed using a one-way ANOVA test. *$P < 0.05$, **$P < 0.01$.

treated mice, and the most marked changes were observed at a concentration of 500 µM (Fig. 7D).

## DISCUSSION

Our work provides evidence regarding the mechanism underlying IL-8–induced NET formation in patients with ocular-active BD. NETs could upregulate proinflammatory cytokines in microglial activation. Pretreatment with an IL-8 receptor antagonist notably ameliorated the production of NETs in EAU mice. Mechanistically, our observations confirmed the influence of IL-8 on NET production via the MAPK/NADPH oxidase pathway.

Consistent with the mounting evidence of the involvement of IL-8 and its functioning receptors CXCR1/2 in BD pathogenesis, our study found that IL-8 expression levels were increased in the serum of patients with ocular-active BD. Concerning the association of IL-8 with NET formation, our study found that IL-8 notably increased NET formation in a dose-dependent manner, indicating that it is indeed a potentially robust inducer of NET formation.

Excessive NETs usually cause inflammation and tissue damage.[31] In addition to ophthalmic diseases, a variety

of cardiovascular, inflammatory, immune, and metabolic diseases are significantly associated with NETs. The inflammatory environment in ulcerative colitis and acute gout encourages neutrophil activation and IL-1 expression.[32] Extracellular MPO exacerbates neutrophil-mediated glomerular damage in crescentic glomerulonephritis.[33] The interaction of lipopolysaccharide with the Toll-like receptor 4 located on neutrophils is a major route leading to the NET formation in lung infection.[34,35] Moreover, Toll-like receptor 4 expression is one of the key potentiators of NET production in chronic obstructive pulmonary disease. Acute lung injury and acute respiratory distress syndrome may be caused by elevated levels of IL-1 and high mobility group box protein 1, both of which have been found to induce NETosis. In patients with Alzheimer's disease, neutrophils have been detected infiltrating the brain parenchyma and releasing NETs, resulting in the death of neuronal cells and damage to the blood–brain barrier.[36]

There are two main mechanisms underlying NET formation, NADPH oxidase dependent and NADPH oxidase independent. Induction of NETosis is related to the activation of NADPH oxidase, the latter of which causes calcium release from intracellular storage, production of ROS, and acti-
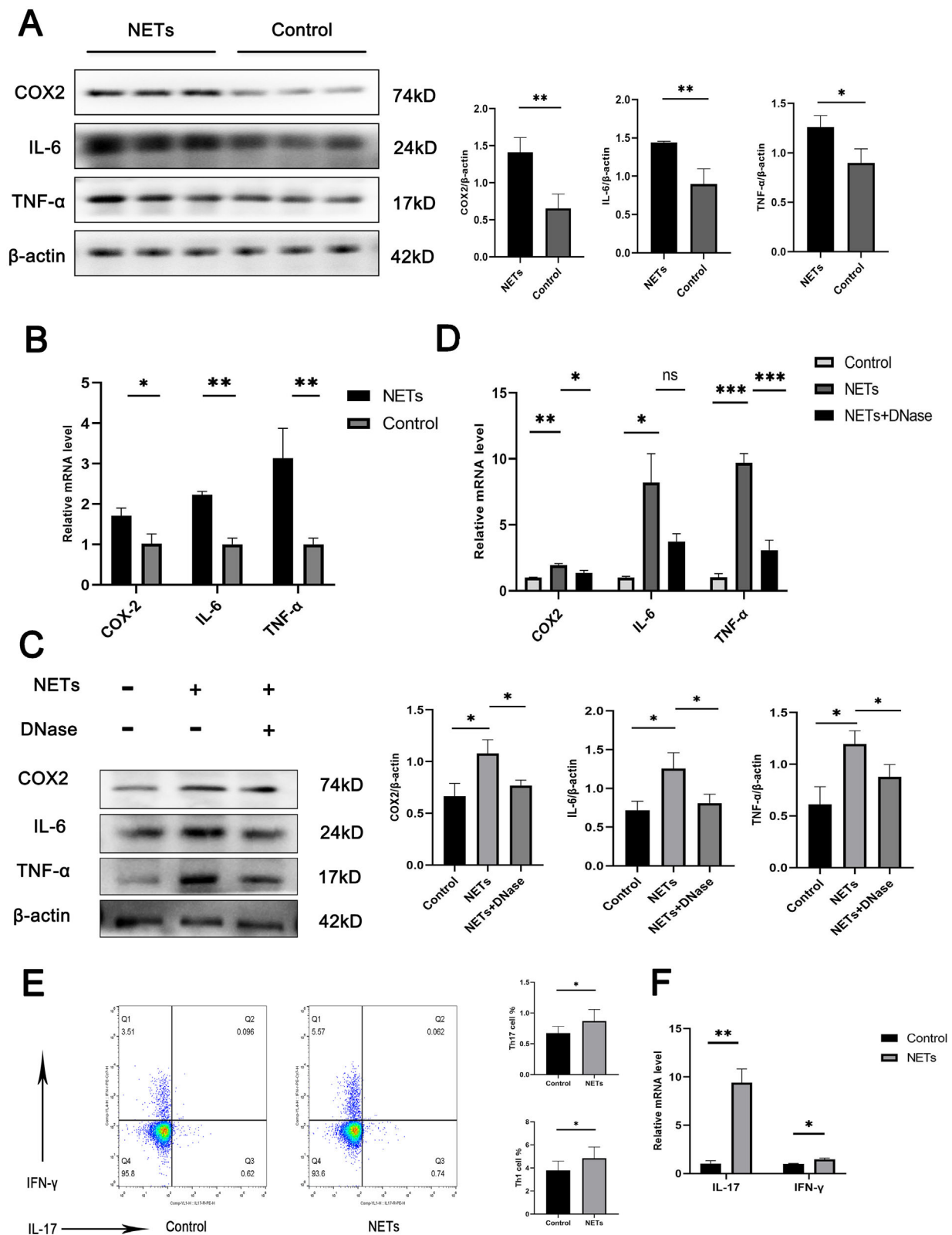
**FIGURE 5.** NETs produced upon IL-8 stimulation promote inflammation in microglia and CD4$^+$ T cells. (**A**) HMC3 cells were treated with NETs 500 (ng/mL) for 24 hours. Western blot assays of COX2, IL-6, and TNF-$\alpha$ expression in HMC3 cells were performed ($n = 3$ per group; unpaired $t$ test). The protein samples were quantified using densitometry through ImageJ software and normalized. (**B**) HMC3 cells were treated with NETs 500 (ng/mL) for 24 hours. RT-qPCR of COX2, IL-6, and TNF-$\alpha$ expression in HMC3 cells was performed ($n = 3$ per group; unpaired $t$ test). (**C**) HMC3 cells were treated with NETs 500 (ng/mL) for 24 hours in the absence or presence of DNase I. Western blot assays of COX2, IL-6, and TNF-$\alpha$ expression in HMC3 cells were performed ($n = 3$ per group; one-way ANOVA test). The protein samples were quantified using densitometry through ImageJ software and normalized. (**D**) HMC3 cells were treated with NETs 500 (ng/mL) for 24 hours in the absence or presence of DNase I. RT-qPCR of COX2, IL-6, and TNF-$\alpha$ expression in HMC3 cells was performed ($n = 3$ per group;

one-way ANOVA test). (**E**) CD4$^+$ T cells were treated with NETs 500 (ng/mL). Representative flow cytometry images of Th1 (IFN-$\gamma^+$CD4$^+$) and Th17 (IL-17A$^+$CD4$^+$) cells. ($n = 3$ per group; unpaired $t$-test). (**F**) CD4$^+$ T cells were treated with NETs 500 (ng/mL). RT-qPCR of IL-17 and IFN-$\gamma$ expression in CD4$^+$ T cells was performed ($n = 3$ per group; unpaired $t$ test). The data were expressed as mean ± SD. *$P < 0.05$, **$P < 0.01$.
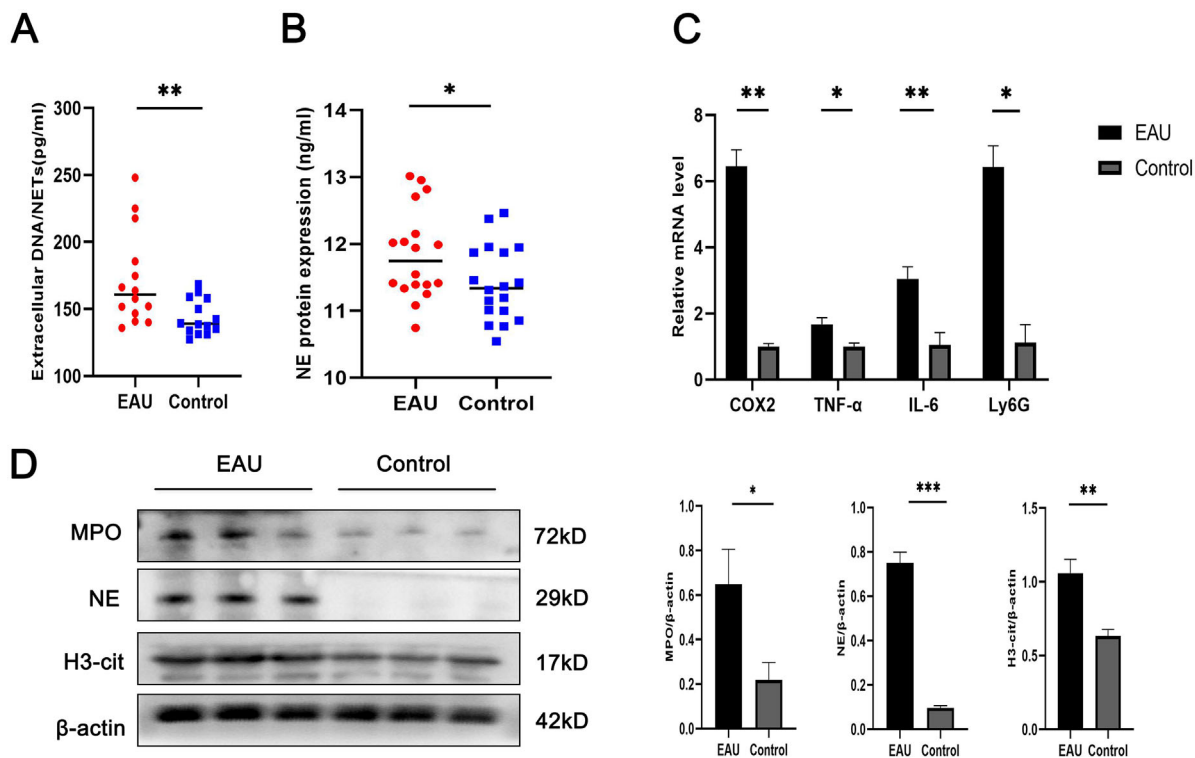


**FIGURE 6.** NET production is increased in EAU mice. (**A**) The levels of extracellular DNA indicated the presence of NETs in EAU mice ($n = 14$ per group). (**B**) The levels of NE indicated the presence of NETs in EAU mice ($n = 18$ per group). (**C**) RT-qPCR of Ly6G, COX2, IL-6, and TNF-$\alpha$ expression in the retinas ($n = 3$ per group). (**D**) Western blot for H3Cit, NE, and MPO expression in retinas ($n = 3$ per group). The protein samples were quantified using densitometry through ImageJ software and normalized. The data were expressed as mean ± SD and analyzed using an unpaired $t$ test. *$P < 0.05$, **$P < 0.01$.

vation of p38 MAPK.[37] The NADPH oxidase-independent mechanism, as a special type, could be triggered by bacteria, such as *Staphylococcus aureus*, without mitochondrial DNA release, which requires the regulation of Toll-like receptors and complement-mediated systems.[38] Our work found the inhibitors of MAPK and NADPH pathways (DPI, SB203580, and PD98059) could decrease the formation of NETs. In our further exploration, our findings confirmed that IL-8–induced NET formation was mediated by the MAPK and NADPH pathways. Therefore, ROS scavengers, such as DNase and *N*-acetylcysteine, could serve as potential therapeutic agents for uveitis.[39]

Microglia-elicited inflammatory processes are involved in the progression of uveitis. Activated microglia release inflammatory factors such as TNF-$\alpha$, IL-1$\beta$, IL-6, and chemokines that recruit peripheral inflammatory cells to the retina.[40] In addition, the excessive inflammatory response from activated microglia may further aggravate inflammation and trigger more retinal damage. Microglial cells, the central nervous system's resident immune cells, can also release extracellular traps.[41] Mice lacking NETs have significantly decreased proinflammatory cytokine levels in the periphery and alleviated neuroinflammation. NET formation in peripheral blood may increase the expression of proinflammatory cytokines that activate brain microglia and trigger neuroinflammation.[42] Given these findings, our study further investigated whether NETs were involved in microglial activation and contributed to microglial inflammation. Our results suggest that NETs exert a proinflammatory effect. The main component of NETs is DNA. Hence, we used DNase I to digest DNA into nonfunctional small fragments to block its effects in NETs and found the proinflammatory effects of NETs were significantly reduced but still stronger than those of the control, suggesting that the DNA in NETs might contribute to inflammation.

It is well-known that T cells play a role in autoimmune diseases or autoinflammatory disease, including BD[7,43] and systemic lupus erythematosus. In a previous study, NETs were found to activate the Th17 cells in patients with psoriasis.[44] In this study, we showed that NETs isolated from neutrophils increased the frequency of Th1/Th17 cells as well as the mRNA expression of IL-17 and IFN-$\gamma$. These results suggest that NETs may exert their effect through activation of Th1/Th17 cells.

EAU is a commonly used model for human uveitis. EAU is characterized by massive infiltration of inflammatory cells
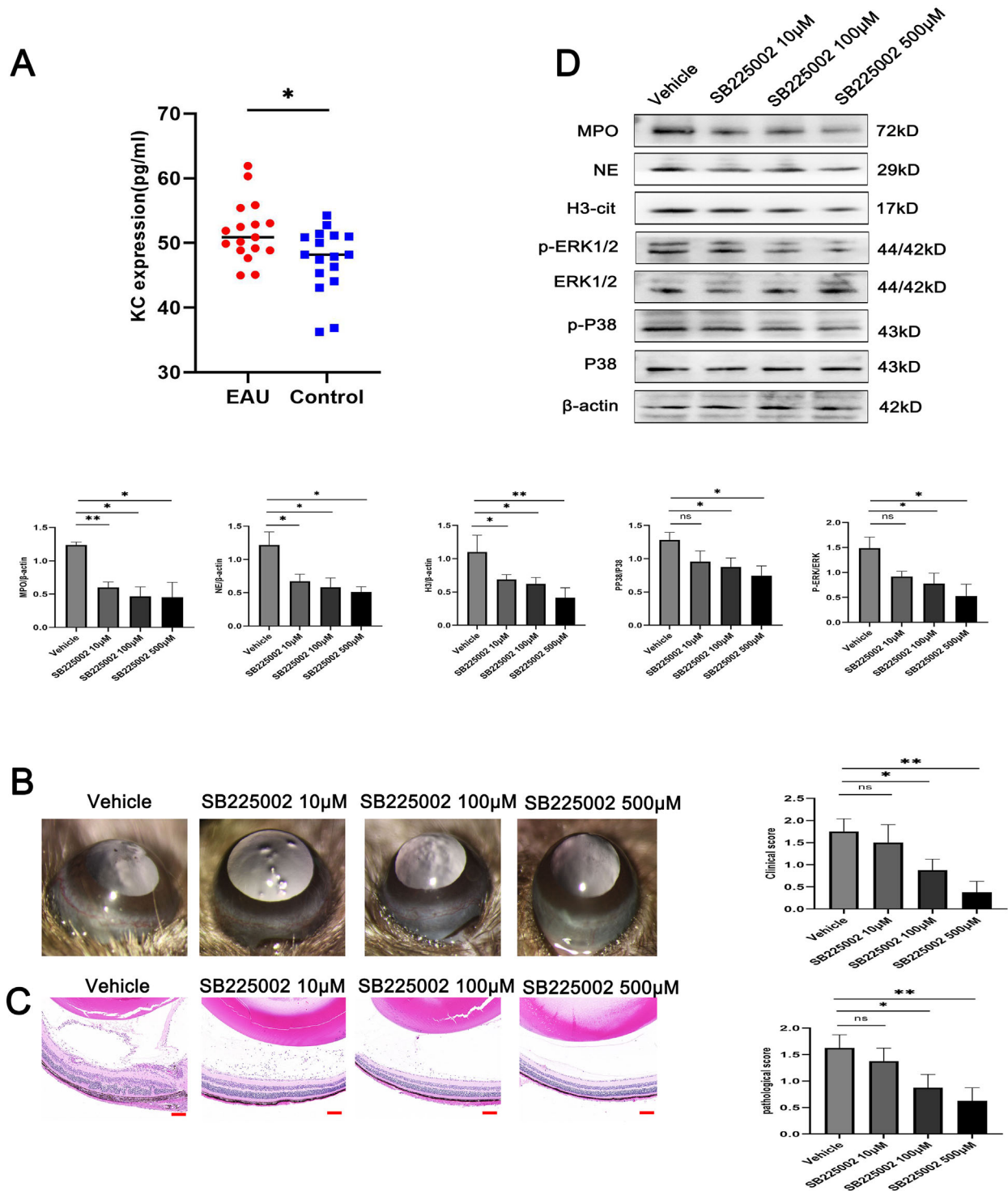
**FIGURE 7.** SB225002 treatment ameliorated the clinical and histological manifestations in EAU mice. (**A**) Comparison of serum KC level between the EAU mice and control mice ($n = 17$ per group; unpaired $t$ test). (**B**) Representative images of the slit lamp (*left*) and quantification of clinical scores (*right*) of the EAU mice treated with the CXCR2 inhibitor SB225002 ($n = 4$ per group; Kruskal–Wallis test). (**C**) Representative images of hematoxylin and eosin staining (*left*) and quantification of histopathological scores (*right*) of the EAU mice treated with the CXCR2 inhibitor SB225002 ($n = 4$ per group; Kruskal–Wallis test; scale bars, 25 µm). (**D**) Western blot for H3Cit, NE, MPO, ERK, p-ERK, P38, and p-P38 expression in retinas ($n = 3$ per group; one-way ANOVA test). The quantification of protein samples was determined via densitometry and normalized. The data were expressed as mean ± SD. *$P < 0.05$, **$P < 0.01$.

such as neutrophils and macrophages in the eyes.[45] According to histological studies in EAU mice, neutrophils have an essential function in tissue destruction that occurs later in the disease.[46] Consistently, we found increased NET secretion and KC levels in EAU mice. Neutrophil infiltration and NET formation cause tissue damage and inflammatory

symptoms in EAU mice. CXCR2 is a chemokine receptor expressed in neutrophils and plays a crucial role in neutrophil recruitment. Brito et al.[47] found that chemokines acting through the IL-8 receptor homolog CXCR2 play an important role in neutrophil infiltration during exdotoxin-induced uveitis. It has been shown that the inhibition of CXCR2 is sufficient to prevent IL-8 and KC-mediated marginalization and chemotaxis of neutrophils to decrease NETosis.[48,49] Our study found that SB225002, a potent and selective CXCR2 antagonist, could highly decrease the disease severity of EAU mice. Studies have shown that SB225002 can affect the occurrence and development of diseases through the MAPK pathway.[50,51] We also observed the intravitreal injection of SB225002 suppressed NET formation and interfered with MAPK signaling. These findings confirmed that IL-8 could induce NET formation via the MAPK pathway. How NETs affect BD development is not yet clear. It is important to continue researching how each NET component interacts with the BD.

In conclusion, our data supported that NET formation was induced by IL-8. The specific mechanism by which IL-8 induces NET formation was found to be related to the MAPK and NADPH pathways. Moreover, pretreatment with the CXCR2 antagonist SB225002 alleviated neutrophil infiltration and suppressed NET formation in EAU mice. Research in our direction may reveal potential new targets or prognostic markers for the treatment of BD or Behçet's uveitis.

### Acknowledgments

Disclosure: **Q. Shu**, None; **N. Zhang**, None; **Y. Liu**, None; **X. Wang**, None; **J. Chen**, None; **H. Xie**, None; **F. Pan**, None; **L. Zhao**, None; **X. Ding**, None; **Y. Wen**, None; **L. Wang**, None; **W. Xie**, None; **J. Lu**, None; **G. Su**, None; **H. Peng**, None; **P. Yang**, None

### References

1. Yang P, Fang W, Meng Q, Ren Y, Xing L, Kijlstra A. Clinical features of Chinese patients with Behçet's disease. *Ophthalmology*. 2008;115:312–318.e314.
2. Tugal-Tutkun I, Ozdal PC, Oray M, Onal S. Review for diagnostics of the year: multimodal imaging in Behçet uveitis. *Ocul Immunol Inflamm*. 2017;25:7–19.
3. Çakar Özdal P. Behçet's uveitis: current diagnostic and therapeutic approach. *Turk J Ophthalmol*. 2020;50:169–182.
4. Yang P, Zhong Z, Du L, et al. Prevalence and clinical features of systemic diseases in Chinese patients with uveitis. *Br J Ophthalmol*. 2021;105:75–82.
5. Yang P, Zhang Z, Zhou H, et al. Clinical patterns and characteristics of uveitis in a tertiary center for uveitis in China. *Curr Eye Res*. 2005;30:943–948.
6. Yang P, Ohno S, Zierhut M. Editorial: new insights into uveitis: immunity, genes, and microbes. *Front Immunol*. 2021;12:765377.
7. Zhong Z, Su G, Kijlstra A, Yang P. Activation of the interleukin-23/interleukin-17 signalling pathway in autoinflammatory and autoimmune uveitis. *Prog Retina Eye Res*. 2021;80:100866.
8. Yamashita N. Hyperreactivity of neutrophils and abnormal T cell homeostasis: a new insight for pathogenesis of Behçet's disease. *Intl Rev Immunol*. 1997;14:11–19.
9. Nakazawa D, Shida H, Kusunoki Y, et al. The responses of macrophages in interaction with neutrophils that undergo NETosis. *J Autoimmun*. 2016;67:19–28.
10. Mutua V, Gershwin LJ. A review of neutrophil extracellular traps (NETs) in disease: potential anti-NETs therapeutics. *Clin Rev Allergy Immunol*. 2021;61:194–211.
11. Tan C, Aziz M, Wang P. The vitals of NETs. *J Leukoc Biol*. 2021;110:797–808.
12. Masuda S, Nakazawa D, Shida H, et al. NETosis markers: quest for specific, objective, and quantitative markers. *Clin Chim Acta*. 2016;459:89–93.
13. Pan B, Alam HB, Chong W, et al. CitH3: a reliable blood biomarker for diagnosis and treatment of endotoxic shock. *Sci Rep*. 2017;7:8972.
14. Thålin C, Daleskog M, Göransson SP, et al. Validation of an enzyme-linked immunosorbent assay for the quantification of citrullinated histone H3 as a marker for neutrophil extracellular traps in human plasma. *Immunol Res*. 2017;65:706–712.
15. Wang L, Zhou X, Yin Y, Mai Y, Wang D, Zhang X. Hyperglycemia induces neutrophil extracellular traps formation through an NADPH oxidase-dependent pathway in diabetic retinopathy. *Front Immunol*. 2018;9:3076.
16. Mahajan A, Hasíková L, Hampel U, et al. Aggregated neutrophil extracellular traps occlude Meibomian glands during ocular surface inflammation. *Ocul Surf*. 2021;20:1–12.
17. Le Joncour A, Martos R, Loyau S, et al. Critical role of neutrophil extracellular traps (NETs) in patients with Behcet's disease. *Ann Rheum Dis*. 2019;78:1274–1282.
18. Li H, Tan H, Liu Z, et al. Succinic acid exacerbates experimental autoimmune uveitis by stimulating neutrophil extracellular traps formation via SUCNR1 receptor. *Br J Ophthalmol*. 2022;28:bjophthalmol-2021-320880.
19. Zeng J, Wu M, Zhou Y, Zhu M, Liu X. Neutrophil extracellular traps (NETs) in ocular diseases: an update. *Biomolecules*. 2022;12:1440.
20. Agarwal RK, Silver PB, Caspi RR. Rodent models of experimental autoimmune uveitis. *Methods Mol Biol*. 2012;900:443–469.
21. Yang JM, Yun K, Jeon J, et al. Multimodal evaluation of an interphotoreceptor retinoid-binding protein-induced mouse model of experimental autoimmune uveitis. *Exp Mol Med*. 2022;54:252–262.
22. Mukaida N, Harada A, Matsushima K. Interleukin-8 (IL-8) and monocyte chemotactic and activating factor (MCAF/MCP-1), chemokines essentially involved in inflammatory and immune reactions. *Cytokine Growth Factor Rev*. 1998;9:9–23.
23. Hu N, Westra J, Rutgers A, et al. Decreased CXCR1 and CXCR2 expression on neutrophils in anti-neutrophil cytoplasmic autoantibody-associated vasculitides potentially increases neutrophil adhesion and impairs migration. *Arthritis Res Ther*. 2011;13:R201.
24. Durmazlar SP, Ulkar GB, Eskioglu F, Tatlican S, Mert A, Akgul A. Significance of serum interleukin-8 levels in patients with Behcet's disease: high levels may indicate vascular involvement. *Intl J Dermatol*. 2009;48:259–264.
25. Sahin S, Akoğlu T, Direskeneli H, Sen LS, Lawrence R. Neutrophil adhesion to endothelial cells and factors affecting adhesion in patients with Behçet's disease. *Ann Rheum Dis*. 1996;55:128–133.
26. Katsantonis J, Adler Y, Orfanos CE, Zouboulis CC. Adamantiades-Behçet's disease: serum IL-8 is a more reliable marker for disease activity than C-reactive protein

and erythrocyte sedimentation rate. *Dermatology (Basel, Switzerland)*. 2000;201:37–39.

27. International Study Group for Behçet's Disease. Criteria for diagnosis of Behçet's disease. *Lancet*. 1990;335:1078–1080.

28. Neels JG, Badeanlou L, Hester KD, Samad F. Keratinocyte-derived chemokine in obesity: expression, regulation, and role in adipose macrophage infiltration and glucose homeostasis. *J Biol Chem*. 2009;284:20692–20698.

29. Wu W, Xu Y, He X, et al. IL-33 promotes mouse keratinocyte-derived chemokine, an IL-8 homologue, expression in airway smooth muscle cells in ovalbumin-sensitized mice. *Asian Pac J Allergy Immunol*. 2014;32:337–344.

30. Bozic CR, Gerard NP, von Uexkull-Guldenband C, et al. The murine interleukin 8 type B receptor homologue and its ligands. Expression and biological characterization. *J Biol Chem*. 1994;269:29355–29358.

31. Yu S, Liu J, Yan N. Endothelial dysfunction induced by extracellular neutrophil traps plays important role in the occurrence and treatment of extracellular neutrophil traps-related disease. *Int J Mol Sci*. 2022;23:5626.

32. Angelidou I, Chrysanthopoulou A, Mitsios A, et al. REDD1/autophagy pathway is associated with neutrophil-driven IL-1$\beta$ inflammatory response in active ulcerative colitis. *J Immunol*. 2018;200:3950–3961.

33. Odobasic D, Kitching AR, Semple TJ, Holdsworth SR. Endogenous myeloperoxidase promotes neutrophil-mediated renal injury, but attenuates T cell immunity inducing crescentic glomerulonephritis. *J Am Soc Nephrol JASN*. 2007;18:760–770.

34. Funchal GA, Jaeger N, Czepielewski RS, et al. Respiratory syncytial virus fusion protein promotes TLR-4-dependent neutrophil extracellular trap formation by human neutrophils. *PLoS One*. 2015;10:e0124082.

35. Sung PS, Peng YC, Yang SP, Chiu CH, Hsieh SL. CLEC5A is critical in Pseudomonas aeruginosa-induced NET formation and acute lung injury. *JCI Insight*. 2022;7:e156613.

36. Pietronigro EC, Della Bianca V, Zenaro E, Constantin G. NETosis in Alzheimer's disease. *Front Immunol*. 2017;8:211.

37. Keshari RS, Verma A, Barthwal MK, Dikshit M. Reactive oxygen species-induced activation of ERK and p38 MAPK mediates PMA-induced NETs release from human neutrophils. *J Cell Biochem*. 2013;114:532–540.

38. Pilsczek FH, Salina D, Poon KK, et al. A novel mechanism of rapid nuclear neutrophil extracellular trap formation in response to Staphylococcus aureus. *J Immunol*. 2010;185:7413–7425.

39. Zhang XY, Hayasaka S, Hayasaka Y, Cui HS, Chi ZL. Effect of N-acetylcysteine on lipopolysaccharide-induced uveitis in rats. *Jpn J Ophthalmol*. 2007;51:14–20.

40. Rathnasamy G, Foulds WS, Ling EA, Kaur C. Retinal microglia - a key player in healthy and diseased retina. *Prog Neurobiol*. 2019;173:18–40.

41. Wu X, Zeng H, Cai L, Chen G. Role of the extracellular traps in central nervous system. *Front Immunol*. 2021;12:783882.

42. Kong Y, He G, Zhang X, Li J. The role of neutrophil extracellular traps in lipopolysaccharide-induced depression-like behaviors in mice. *Brain Sci*. 2021;11:1514.

43. Chi W, Yang P, Zhu X, et al. Production of interleukin-17 in Behcet's disease is inhibited by cyclosporin A. *Mol Vis*. 2010;16:880–886.

44. Lambert S, Hambro CA, Johnston A, et al. Neutrophil extracellular traps induce human Th17 cells: effect of psoriasis-associated TRAF3IP2 genotype. *J Invest Dermatol*. 2019;139:1245–1253.

45. Sonoda KH, Yoshimura T, Egashira K, Charo IF, Ishibashi T. Neutrophil-dominant experimental autoimmune uveitis in CC-chemokine receptor 2 knockout mice. *Acta Ophthalmol*. 2011;89:e180–188.

46. Kerr EC, Raveney BJ, Copland DA, Dick AD, Nicholson LB. Analysis of retinal cellular infiltrate in experimental autoimmune uveoretinitis reveals multiple regulatory cell populations. *J Autoimmun*. 2008;31:354–361.

47. Brito BE, O'Rourke LM, Pan Y, et al. Murine endotoxin-induced uveitis, but not immune complex-induced uveitis, is dependent on the IL-8 receptor homolog. *Curr Eye Res*. 1999;19:76–85.

48. White JR, Lee JM, Young PR, et al. Identification of a potent, selective non-peptide CXCR2 antagonist that inhibits interleukin-8-induced neutrophil migration. *J Biol Chem*. 1998;273:10095–10098.

49. Alsabani M, Abrams ST, Cheng Z, et al. Reduction of NETosis by targeting CXCR1/2 reduces thrombosis, lung injury, and mortality in experimental human and murine sepsis. *Br J Anaesthes*. 2022;128:283–293.

50. Goda AE, Koyama M, Sowa Y, et al. Molecular mechanisms of the antitumor activity of SB225002: a novel microtubule inhibitor. *Biochem Pharmacol*. 2013;85:1741–1752.

51. Wang X, Sun L, He N, et al. Increased expression of CXCL2 in ACPA-positive rheumatoid arthritis and its role in osteoclastogenesis. *Clin Exp Immunol*. 2021;203:194–208.